AIP | The Journal of Chemical Physics

The possible equilibrium shapes of static pendant drops

P. T. Sumesh and Rama Govindarajan

Citation: The Journal of Chemical Physics **133**, 144707 (2010); doi: 10.1063/1.3494041
View online: http://dx.doi.org/10.1063/1.3494041
View Table of Contents: http://scitation.aip.org/content/aip/journal/jcp/133/14?ver=pdfcov
Published by the AIP Publishing

The possible equilibrium shapes of static pendant drops

P. T. Sumesh and Rama Govindarajan[a)]
Engineering Mechanics Unit, Jawaharlal Nehru Centre for Advanced Scientific Research, Jakkur, Bangalore 560064, India

(Received 6 May 2010; accepted 7 September 2010; published online 12 October 2010)

Analytical and numerical studies are carried out on the shapes of two-dimensional and axisymmetric pendant drops hanging under gravity from a solid surface. Drop shapes with both pinned and equilibrium contact angles are obtained naturally from a single boundary condition in the analytical energy optimization procedure. The numerical procedure also yields optimum energy shapes, satisfying Young's equation without the explicit imposition of a boundary condition at the plate. It is shown analytically that a static pendant two-dimensional drop can never be longer than 3.42 times the capillary length. A related finding is that a range of existing solutions for long two-dimensional drops correspond to unphysical drop shapes. Therefore, two-dimensional drops of small volume display only one static solution. In contrast, it is known that axisymmetric drops can display multiple solutions for a given volume. We demonstrate numerically that there is no limit to the height of multiple-lobed Kelvin drops, but the total volume is finite, with the volume of successive lobes forming a convergent series. The stability of such drops is in question, though. Drops of small volume can attain large heights. A bifurcation is found within the one-parameter space of Laplacian shapes, with a range of longer drops displaying a minimum in energy in the investigated space. Axisymmetric Kelvin drops exhibit an infinite number of bifurcations. © *2010 American Institute of Physics*. [doi:10.1063/1.3494041]

I. INTRODUCTION

Often, one encounters pendant drops hanging from an infinite solid surface. However, the body of work on this geometry is far smaller than on drops hanging from a support of fixed radius or from an orifice. In contrast to sessile drops that can be made as large as one would wish, a pendant drop larger than a certain volume cannot hang in a stationary fashion, as we will demonstrate. Interestingly, while sessile drops can be no taller than twice their capillary length, we will see that pendant drops can be infinitely tall, in theory. Thus, an infinite number of shapes of pendant drops are possible for a given volume. A generalized boundary condition applicable in several situations is presented. Such shapes are obtained numerically without the explicit imposition of boundary conditions at the solid plate.

We begin by briefly discussing some of the earlier studies on this problem. Using calculus of variations, Gauss, in 1830, unified the results of Young and Laplace to obtain equations and boundary conditions describing drop shapes,[1] while Plateau[2] classified the solutions of the gravity-free Young–Laplace equation according to geometry. Adam and Bashforth[3] obtained gravity-distorted drop shapes. Kelvin[4] geometrically constructed menisci including the multiple-lobed pendant drops now known by his name. We go forward by almost a century to early numerical simulations, important among which are those of Padday,[5] for axisymmetric sessile and pendant drops and liquid bridges. Padday and Pitt[6] calculated axisymmetric equilibrium shapes from the first variation of energy and graphically examined their stability through the second variations of energy. More formal calculations followed, from Pitts,[7,8] who derived the shape and stability of two-dimensional and axisymmetric pendant drops for various contact angles and showed that there is a maximum in the volume that can be sustained. He showed that drops are unstable in a regime where an increase in volume is associated with a decrease in height. Boucher *et al.*[9,10] carried out a similar analysis on pendant and sessile drops and emergent and captive bubbles. They explored the relationship between shape and contact-angle hysteresis. Many properties of the solutions, including of Kelvin drops, were elucidated by Concus and Finn.[11]

Meanwhile, Michael and co-workers[12–14] conducted a systematic analysis of the stability of two-dimensional drops hanging from a fixed support or fixed orifice and axisymmetric drops hanging from a fixed tube, which are discussed in Sec. III D. Wente[15] carried out rigorous mathematical investigations whose conclusions include (i) that the drop height increases monotonically with volume throughout the range of stability, in agreement with Pitts;[8] (ii) that the area of contact of the drop with the solid surface attains a maximum before the volume does; and (iii) that the profile curve of a stable pendant drop never contains more than one inflection point.

Chesters[16] attempted to calculate the shape of a pendant drop hanging from a tube as a first-order perturbation to a circle. This approach was revisited by O'Brien[17] with an al-

[a)]Electronic mail: rama@jncasr.ac.in.

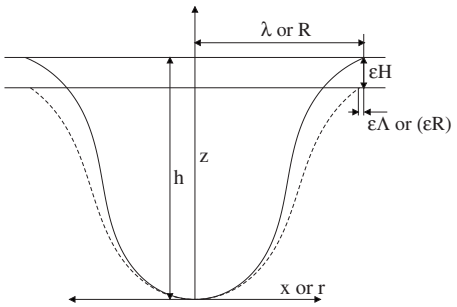

FIG. 1. Definition of coordinate system (x,z) for two-dimensional and (r,z) for axisymmetric pendant drops. The perturbed shape is shown by the dashed line.

ternate formulation. Through the introduction of different scaling and boundary layers, the shape of a pendant drop was calculated using matched asymptotic expansions. Later on, O'Brien[18] extended the theory to pendant drops with multiple necks (Kelvin's drops).

The recent approach of Snoeijer and Andreotti[19] for sessile drops is particularly similar to the present, i.e., posing the problem with free end points. By using a similar approach on pendant drops, we find that these can be much more interesting than sessile. In particular, they can have multiple minimum energy shapes at a given volume. Moreover, they have a different energy landscape, as we shall see. To the best of our knowledge, studies of pendant drops hanging from solid surfaces, which obtain shapes through an energy minimization procedure, all hold a fixed area of contact with the solid. Correct drop shapes are then obtained by additionally imposing Young's relation at the solid surface. In contrast, we fix only one parameter rather than two and allow the second to come out of the solution. We could do this in many ways, e.g., by keeping the volume fixed and allowing the contact area to change or by keeping the contact area fixed and allowing the volume to change. We choose the former since it is natural and many features such as multiple shapes are obtained directly rather than by an exhaustive search. Drop shapes obeying Young's relation emerge naturally in our procedure.

II. DROP SHAPES OF MINIMUM AND MAXIMUM ENERGY

We study both two-dimensional and axisymmetric drops. The shape of a two-dimensional drop, i.e., an infinite cylinder whose cross-section is a drop, is possible to obtain analytically, whereas axisymmetric drops warrant numerical computations. Since the analytical solution is often instructive, we study two-dimensional drops as well, although one may not often encounter them in reality, except as remnants of inverted rivulets and in some small-scale situations.

Consider a liquid drop suspended downward from a horizontal solid surface, subjected to gravity and surface forces. For a given drop volume, we begin by obtaining shapes for which the energy is at an optimum. The solid-liquid contact area is not predefined nor is the contact line pinned. As sketched in Fig. 1, the bottom tip of the drop is taken to be the origin of the coordinate system, with the vertical coordinate z increasing upward. The shape of the liquid-gas interface is described by $x(z)$ or $r(z)$, where x for a two-dimensional drop is the horizontal distance of the liquid-gas interface from the z-axis and r is the corresponding radial distance for an axisymmetric drop. Following Pitts,[7,8] we write

$$E_0 = \int_0^h [\gamma\sqrt{1+x_z^2} - \rho g x(h-z)]\mathrm{d}z + (\gamma_{sl} - \gamma_{sg})\lambda, \qquad (1)$$

where the total energy for a two-dimensional drop is $2E_0$ per unit span. The solid plate is taken to be the base for potential energy. The drop is characterized by its total height h and the solid-liquid interface half-length λ. The liquid density is ρ, while γ, γ_{sl}, and γ_{sg}, respectively, are the tensions of the liquid-gas, liquid-solid and solid-gas interfaces. We nondimensionalize the above equation by the capillary length $L_c \equiv \sqrt{\gamma/\rho g}$ as the length scale and γL_c as the two-dimensional energy scale. The functional E_0 must be extremized subject to the constraint of constant volume V.

Here we note one point of departure from earlier works.[7,10] Whereas those studies specified the liquid-gas interfacial contact length 2λ to be held constant during the minimization procedure, thus making the contact line pinned in effect, we do not (as we should not for our problem!) impose this additional constraint. In a typical problem of this class, with the end point held fixed, one would need to specify an additional boundary condition at this point. Thus, in order to completely specify the shape, earlier studies imposed the equilibrium angle θ_e at the surface, where θ_e is given by Young's equation

$$\gamma_{sl} - \gamma_{sg} + \gamma\cos\theta_e = 0. \qquad (2)$$

On the other hand, with the end point allowed to move, no additional information needs to be supplied,[20] so our approach holds appeal in that the class of solutions of extremum energy that we obtain automatically have Young's contact angle θ_e. Also, some additional features of the solution space are revealed as we shall see below.

We consider a perturbed shape $\hat{x}=x+\epsilon\eta(z)$ where ϵ is a small parameter. We prescribe that the bottom tips of the perturbed and the original drops coincide, as seen in Fig. 1. Since the problem involves free end points, let the corresponding changes in the end points be $[\hat{\lambda}=\lambda+\epsilon\Lambda,\ \hat{h}=h+\epsilon H]$. As detailed in the Appendix, a standard energy minimization procedure gives the Euler–Lagrange equation

$$z - \frac{1}{r_0} = \frac{\mathrm{d}}{\mathrm{d}z}\left(\frac{x_z}{\sqrt{1+x_z^2}}\right) \qquad (3)$$

and the boundary condition

$$\frac{\epsilon\Lambda}{\epsilon H}\left(\cos\theta_s + \frac{\gamma_{sl}-\gamma_{sg}}{\gamma}\right) = 0, \qquad (4)$$

where $\cot(\theta_s)$ is the slope x_z at the solid surface.

The Euler–Lagrange equations offer a static drop shape for every r_0, so we reduce the solution space to a one-dimensional space in the Lagrange multiplier, all of which ensure force balance everywhere.[19] Shapes of minimum or maximum energy among static shapes may then be picked

from these. This property is exploited in Sec. III A to adopt a numerical approach. This approach is more elegant than looking for minimum energy shapes by making arbitrary perturbations which may not satisfy force balance, such as that of Pitts,[7] where the curvature at the bottom was not disturbed. Pitts's procedure would result in a minimum energy for any trial shape, but a class of correct shapes was obtained by imposing Young's contact angle at the surface. However, while the present analytical procedure yields correct extremum energy shapes, we resolve the issue of whether the energy of such shapes is at a maximum or a minimum numerically. Care must be exercised in interpreting these results in terms of stability, as discussed later.

The above general boundary condition [Eq. (4)] offers two possibilities corresponding to actual static drop shapes. (i) If we set the quantity within the brackets to zero, we see that θ_s is equal to the equilibrium contact angle θ_e, to the automatic satisfaction of Young's Eq. (2) of local surface tension balance. We refer to these as Y solutions. (ii) If the contact line is pinned due to surface roughness or chemical heterogeneities, then by definition $\epsilon\Lambda=0$, illustrating that drops sitting on nonideal surfaces need not satisfy Young's equation at the contact line. The explanation usually offered for static drops not satisfying Young's equation is that of contact-angle hysteresis.[21] Wall roughness is particularly simple to imagine as a cause for hysteresis: the fluid at the triple-contact line adjusts its location very slightly to choose a point on the surface where the microscopic angle is θ_e, while maintaining the macroscopic angle at a different θ_s. Moreover, since the curvature at any height z is uniquely determined by r_0, the perturbed solution cannot cross the original one, i.e., $\eta(z)$ cannot change sign in a given shape. This implies that to attain a volume V, the perturbed drop must be taller if the perturbation in r_0 is negative and shorter if otherwise, so H cannot be zero.

These conclusions are easily extended to axisymmetric pendant drops. The energy functional of an axisymmetric drop with height h and liquid-solid contact radius R, defined in a coordinate system (r,z) (Fig. 1), when perturbed to a nearby function $\hat{r}=r+\epsilon\eta$ with the end point moving to $[\hat{R}=R+\epsilon\Omega,\ \hat{h}=h+\epsilon H]$, we obtain the Euler–Lagrange equation describing the shape of drop as

$$z-\frac{1}{r_0}=\left[\frac{r_{zz}}{(1+r_z^2)^{3/2}}-\frac{1}{r(1+r_z^2)^{1/2}}\right] \tag{5}$$

and the end-point condition

$$\frac{\epsilon\Omega}{\epsilon H}\left(\cos\theta_s+\frac{\gamma_{sl}-\gamma_{sg}}{\gamma}\right)=0. \tag{6}$$

Again we obtain Y and pinned solutions by setting different terms in Eq. (6) to zero.

We have not yet resolved whether the solutions obtained correspond to maxima or minima in energy. We do this numerically, as discussed in Sec. III, where other features also come to light.

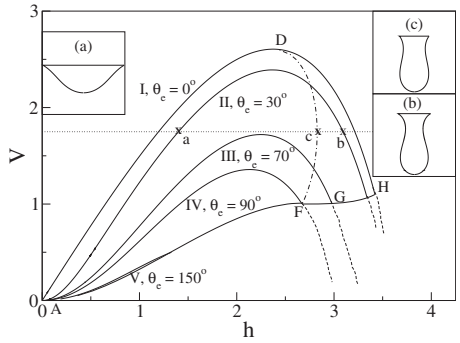

FIG. 2. Volume of extremum energy shapes as a function of height for 2D drops. Curves I–V correspond to Y solutions of different contact angles. Points below AFGH, including the dashed lines of Pitts (Ref. 7), have unphysical drop shapes. Drop shapes shown in the insets correspond to the heights indicated by "a," "c," and "b," all with a volume $V=1.75$. The shape c sits on the dotted-dashed curve FD discussed in Sec. III D.

III. RESULTS AND DISCUSSION

A. Two-dimensional drops

Equation (3) may be integrated[22] to give

$$\frac{dz}{dx}=\left[\frac{1}{(1-(z/r_0)+0.5z^2)^2}-1\right]^{1/2}. \tag{7}$$

The shape for each r_0 is obtained by numerically integrating Eq. (7) by a fourth order Runge–Kutta method and placing the solid surface at the height h where the volume V is attained. Here, the entire space of shapes has been reduced to a one-parameter space in r_0 since we know that any two-dimensional or axisymmetric shape outside this family cannot satisfy force balance which is a necessary condition for an energy minimum. The liquid-gas and liquid-solid interfacial areas and the center of mass of the shape were determined and used to calculate the surface energy and potential energy, respectively. The total energy is then obtained as a function of the shape factor r_0^2 and a line search is employed to obtain the minimum energy solutions along r_0 for each given volume. These solutions are shown in Fig. 2 in a height-volume space. Note that the shape of a drop is independent of interfacial tensions, but its energy depends on their combination, appearing through θ_e. As in the analytical calculations, the boundary conditions were never enforced, but they emerged naturally during the minimization procedure.

In Fig. 2, curves I–V show present extremum energy solutions whose contact angle θ_s turns out to be equal to θ_e, and which therefore belong to the Y branch. These lines agree very well with those obtained by Pitts[7] by imposing Young's contact angle at the solid surface, except that Pitts obtained two solutions for every volume, while the present solutions terminate at the curve AFGH. Any point below this curve corresponds to unphysical shapes which cross themselves, so we find that at low volumes only one solution exists. Note that for contact angles close to 90°, the unphysical solutions (dashed lines) extend over a significant region. The curve AF corresponds to limiting shapes where the drop crosses itself at the solid surface, i.e., the contact area λ is zero, whereas drops on the curve FGH attain a zero width at

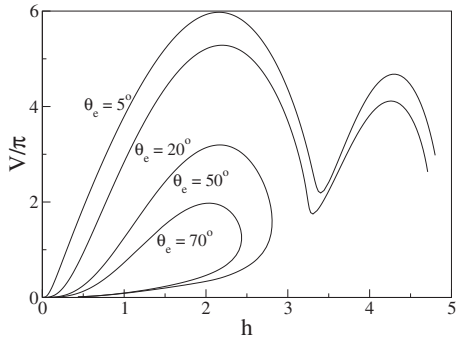

FIG. 3. Volume vs height for extremum energy axisymmetric pendant drops of the Y class obtained during the numerical minimization of energy along with other solutions. Note that the condition $\theta_s=\theta_e$ was not explicitly imposed.

some $z \neq h$. We thus conclude that all possible physical two-dimensional drop shapes are contained within the closed region AFGHD0A.

B. Axisymmetric pendant drops

Following Boucher,[9] Eq. (5) is converted into three coupled first-order equations with θ, r, and z as parameters dependent on s, the arc length from the origin,

$$\frac{d\theta}{ds} = \frac{1}{r_0} - z - \frac{\sin\theta}{r}, \tag{8}$$

where $dr/ds=\cos\theta$ and $dz/ds=\sin\theta$. This approach avoids zero and infinite slopes in the computation.

The same numerical procedure as for two-dimensional drops was adopted here too. Similar conclusions are arrived at, with the important difference that many shapes are possible for a given volume. In fact, in some range of volumes, one can have an infinite number of possible shapes displaying minimum energy. This is because the azimuthal curvature is now finite, ensuring that the drop never intersects itself. The $V-h$ profile of the shortest few of these drops is shown in Fig. 3. The first Y limb and a part of the second at low θ_e were already obtained by Pitts,[8] but again by pinning R and imposing θ_e.

Unlike in the two-dimensional case, at higher θ_e, one may have closed curves in the height-volume space; two examples are seen in Fig. 3. A very large number of such closed curves are possible (not shown). These are remarkable because they represent another basic difference between possible shapes for two-dimensional and axisymmetric drops: axisymmetric drops of small volume can be very long. The second curvature also provides the facility for the longitudinal curvature to be nonmonotonic, so many-lobed, or Kelvin, drops are possible. Of course these shapes may or may not be stable.

C. Height of pendant drops

We show analytically that two-dimensional drops can never be taller than 3.42 times the capillary length. We then show numerically that the height of an axisymmetric drop has no limit, but its volume is always finite.

For two-dimensional drops, Eq. (7) can be written as

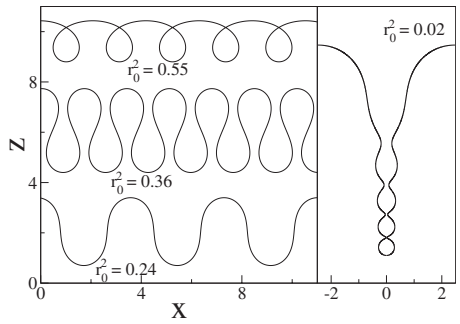

FIG. 4. Solutions of Eq. (3) for various values of r_0 for two-dimensional drops. Once an r_0 is fixed, the only possible shapes for any volume are dictated by the curves on the left. Thus, to obtain a shape for a given volume, one merely draws a horizontal cut on the curve to enclose the desired volume. Shown on the right is a typical Kelvin drop, solution of Eq. (5).

$$z = \frac{1}{r_0} + \left[\frac{1}{r_0^2} - 4\sin^2\left(\frac{\theta_s}{2}\right)\right]^{1/2} \tag{9}$$

so the maximum height $h_{max}=2/r_0$ occurs when $\theta_s=0$. On examining Eq. (7) by putting the numerator and denominator to zero separately to obtain the locations of zero and infinite slopes for z_x, one can deduce that (Fig. 4) (i) when $0 \leq r_0 \leq 0.5$, moving upward in z, θ will go through $\pi/2$ followed by a zero, without a neck, (see $r_0^2=0.24$ in Fig. 4); (ii) when $0.5 \leq r_0 \leq \sqrt{0.5}$ between two points where $\theta=\pi/2$, a saddle point will exist. These are followed by $\theta=0$, so a neck is seen, (see $r_0^2=0.36$ in Fig. 4); and (iii) when $\sqrt{0.5} \leq r_0$, the drop reaches zero slope with out going through any infinite slope. (see $r_0^2=0.55$ in Fig. 4). For all cases, z_x has zeros at $z=0$ and $z=2/r_0^2$. In case of (i), z_x has additional zeros at $z=(1 \pm \sqrt{1-4r_0^2})/r_0$ and no drop can be taller than the lesser of these, which restricts the drop to $h \leq 2$. Hence arbitrarily small r_0 does not suggest arbitrarily tall drops. Also, self-crossing drops are not real solutions and should be excluded from consideration, which has often been overlooked.[7,14] In cases (ii) and (iii), a zero would occur at $z \leq 8$, but the self-crossing condition occurs at a lower height, as seen below. Equation (3) may be integrated[7] to give

$$x = \mp \frac{1}{r_0}[(2r_0^2 - 1)u + E(u|4r_0^2)], \tag{10}$$

where $u=F\left(\frac{\theta}{2}\middle|4r_0^2\right)$ and F and E denote, respectively, elliptic integrals of the first and second kind. The tallest drop is one which barely grazes itself, i.e., achieves $x=0$ with $\theta=\pi/2$ at $x=0$. Equation (10) can be solved to yield $r_0^2=0.3419$ for such a drop, so $h_{max}=2/r_0=3.420$ is the maximum height possible for a two-dimensional drop. This value matches very well with the numerical height at point H in Fig. 2. The calculations were repeated for various θ_s using MATHEMATICA to generate the curve FGH in Fig. 2.

A typical shape of a Kelvin drop in also shown in Fig. 4 and possible solutions up to some height for Kelvin drops of $\theta_e=30°$ are shown in Fig. 5. A larger h corresponds to a smaller r_0, enabling the drop to sustain larger hydrostatic pressures. At every neck, $\theta=90°$, so at the jth neck, Eq. (5) yields

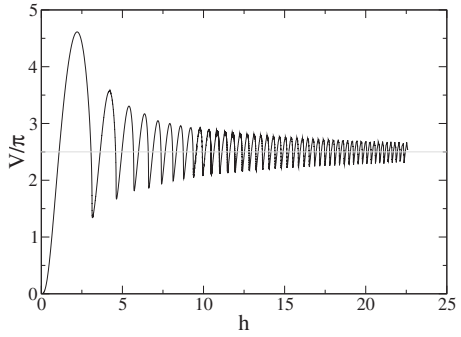

FIG. 5. Kelvin's drop solutions for $\theta_e=30°$ illustrating the existence of multiple configurations for certain volumes.

$$r_{nj}(1 - r_0 z_{nj}) = r_0. \tag{11}$$

Here, the suffix "n" denotes the neck. This shows that each bulge is uniquely determined by r_0 and j, i.e., there is no similarity solution relating consecutive bulges. O'Brien[18] calculated the first few bulges through asymptotic matching.

While it is evident that the volume tends to converge at about 2.5π, Fig. 5 does not make it clear whether the height is converging as well. Figure 6 shows the variation of h_h and h_l (heights at the highs and lows in volume, respectively) with the index j of the Y cycle. Both grow as $j^{1/2}$, so there is no limit on the height of an axisymmetric drop, although the ratios of consecutive heights $h_{h(j+1)}/h_{hj}$ and $h_{l(j+1)}/h_{lj}$ tend toward unity. On comparing drops with j bulges and one with $j+1$, we see that the contribution to the height of each consecutive bulge is $j^{-1/2}$. The radius of each consecutive bulge also goes down roughly on this scale, so the volume of each additional lobe is $\sim j^{-3/2}$. The total volume of the drop is thus given by a convergent series, ensuring that it is finite.

D. Stability and minimum contact area shapes

As detailed in the introduction, the stability analysis of two-dimensional drops has been carried out by various authors.[8,12] The region to the left of the volume maxima in Fig. 2 is found to correspond to energy minima, whereas it is believed that the region to the right of the volume maxima consists of shapes unstable to two-dimensional perturbations. The line joining the maxima in the $V-h$ plane, shown in Fig.

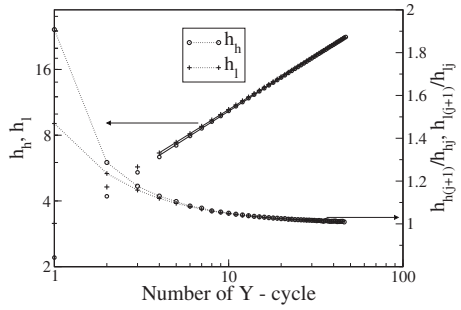

FIG. 6. Heights of Kelvin drops corresponding to highs and lows in volume as a function of the index of the Y cycle. Symbols correspond to drop shapes, while the solid lines are best fits $h_h=3.2j^{0.508}$ and $h_l=3.3j^{0.497}$ The ratio of successive heights on the secondary y-axis is seen to asymptotically approach unity.

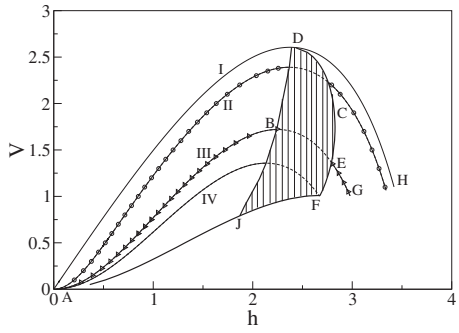

FIG. 7. Possible energy minimum solutions for a two-dimensional drop; the curves' labels are the same as in Fig. 2. The shaded area between the maxima in volume and the MCA is excluded since it consists of energy maxima. Energy minimum solutions for $\theta_e=30$ and 70° are indicated by symbols.

7 by DBJ, is thus a locus of bifurcation points separating stable and unstable solutions. This, however, as we show below, is not the only bifurcation possible.

Before that, a word of caution about the present procedure is in order. Our analytical procedure ensures that the possible shapes we have obtained are all of optimum energy. About the stability of these optimum energy shapes, however, we can only obtain a partial answer from our numerical procedure. This is because, for a given θ_e, we restrict our investigations to a one-dimensional space of all possible Laplacian shapes. When we obtain a maximum in the energy, we can be sure that the shape is unstable. However, a minimum in energy does not ensure stability, since there is a possibility of non-Laplacian shapes of lower energy, i.e., the shape could be dynamically unstable. Second, the drops may be unstable to nonsymmetric perturbations. Michael *et al.*[12] showed that two-dimensional drops hanging from a fixed support could be unstable to three-dimensional perturbations. Such a study needs to be conducted for drops hanging from an infinite solid plate.

1. Two-dimensional shapes

Although Pitts mentioned that some range of longer drops appeared stable, he felt that the result was false due to the very restrictive assumptions he made about the nature of the perturbations. Without his assumptions we obtain a regime of energy minima among long drops. Consider curve III, for example, in Fig. 7. A computation of the energies shows that the left limb AB consists of energy minima, in accordance with accepted wisdom. However, only a portion of BEG, namely, BE, contains energy maxima, whereas the leg EG consists again of energy minima. At any other contact angle as well, the picture is similar, with unstable static shapes to the right of the maximum volume solution, up to the curve FECD, to the right of which we again obtain energy minima. The curve FECD thus describes another locus of bifurcation points. This curve also corresponds to shapes with a minimum in contact area (MCA) subtended at the solid surface. In other words, if we consider all shapes along a horizontal line in Fig. 7, i.e., all shapes of a given volume, the shape with the smallest λ will occur at the intersection of the horizontal line with the curve FECD. This can be seen

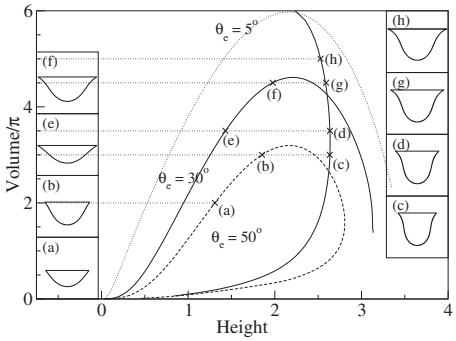

FIG. 8. Typical shapes of axisymmetric drops. (a) $V=2\pi$, $\theta_e=50°$, (b) $V=3\pi$, $\theta_e=50°$, (e) $V=3.5\pi$, $\theta_e=30°$, and (f) $V=4.5\pi$. Shapes subtending a minimum in contact area are shown in (c) $V=3\pi$, $\theta_e=45.2°$, (d) $V=3.5\pi$, $\theta_e=39.1°$, (g) $V=4.5\pi$, $\theta_e=26.8°$, and (h) $V=5\pi$, $\theta_e=20.7°$.

visually in the drop shapes for $V=1.75$ shown in Fig. 2. We may thus summarize by dividing the energy landscape into four sections for a given Young contact angle. (i) The region to the left of the maximum in the $V-h$ plot, i.e., height increases with increasing volume, corresponds to minimum energy shapes. (ii) Shapes in the region lying between the maximum in the $V-h$ plane and the MCA shape on FECD, i.e., the shaded region in Fig. 7 correspond to energy maxima. Here the height decreases with increasing volume and so does the contact area at the solid surface. (iii) The region contained within FECDHGF again consists of energy minimum shapes. In this region, the height decreases with increasing volume, but the contact area with the solid increases. The stability of these shapes to dynamics perturbations needs to be investigated. (iv) The region below AFGH consists of unphysical shapes.

2. Axisymmetric shapes

Typical shapes for axisymmetric drops are illustrated in Fig. 8. The repeating pattern of limbs (Figs. 3 and 5) suggests the existence of more than one set of bifurcations. In fact, each pair of limbs is associated with a minimum contact area locus, which also bifurcates the neighborhood as before; this is confirmed in Fig. 9. Since we find regions of static

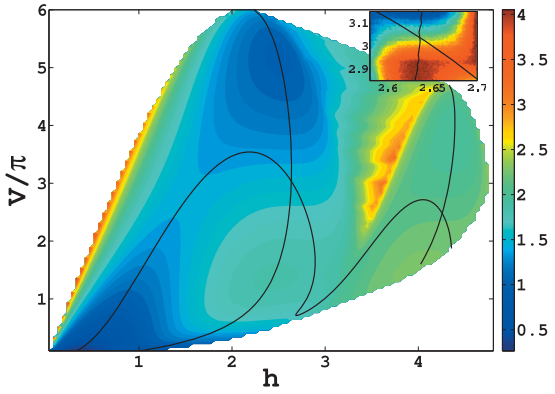

FIG. 9. Energy landscape in height-volume space for $\theta_e=45°$. Deep red corresponds to hills (energy maxima) and deep blue to valleys (minima). The neighborhood of the bifurcation point is enlarged in the inset showing an exchange of stabilities. For ease of visualization, the energy in the inset is normalized between 0 and 1 for each volume.

stability at all Y indices, it is intriguing why we do not see Kelvin's drops in nature. Apart from dynamic instability, since the energy wells are progressively shallower for increasing index, nonlinearities can become important. Thus the presence of extraneous forces, even if small, could play spoilsport, especially at the extremely narrow neck regions. Three-dimensional drops offer an additional possibility of nonaxisymmetric shapes arising from the extra degree of freedom to choose two different radii of curvature at the origin. However, we, following the literature,[6,8] make the hypothesis that the symmetry of the problem should be reflected in the solutions as well and that nonaxisymmetric shapes are less likely minimum energy candidates. Detailed studies on stability to nonaxisymmetric perturbations are perhaps warranted now to prove this point and an ongoing effort is directed at these. Such studies have so far been restricted to pinned/fixed contact area pendant drops.[14] For example, Michael *et al.*[13] showed that ahead of the maximum in volume, axisymmetric drops hanging from a tube are stable to axisymmetric and nonaxisymmetric perturbations below a contact radius of 3.219. We expect that drops hanging from an infinite solid plate, being able to take up the most favorable contact area, are likely to be more stable to nonaxisymmetric perturbations.

3. A word of caution

We notice that Eq. (4) can also be satisfied if $\epsilon\Lambda=0$, i.e., if we restrict ourselves to a special class of perturbations which contain no terms of $O(\epsilon)$ in λ, i.e., when λ is at an extremum. Since one can always create a perturbation that contains terms of this order, the minimum energy shapes thus obtained would be spurious. In fact, the entire MCA curve FECD would correspond to spurious energy extremum shapes for any surface tension because by definition, MCA has a minimum area and no terms of $O(\epsilon)$ exists in λ.

A final word on pinned solutions. Equation (1) is of the form $\int I dz + a \times b = 0$, where the integrand I and the product, given by Eq. (4), have to each vanish. Looking for a pinned solution with a particular λ will give us only the condition on I, leading to a contact angle usually different from θ_e. Several authors[7,9] have in effect arrived at these shapes and, by imposing $b=0$ by hand, obtained the Y solutions. However, we do not have any externally imposed conditions and recover all these solutions. Also, pinned solutions are the result of macroscopic energy minimization where the only relevant length scale is the capillary length. At smaller length scales, intermolecular interactions manifest themselves in various ways at the contact line and a generalized Young's equation may be adopted.[23,24]

IV. SUMMARY

A general energy minimization procedure is adopted for studying static shapes of two-dimensional and axisymmetric pendant drops supported by a solid wall. From this, drops with both (i) pinned contact lines and (ii) equilibrium contact-angle solutions emerge naturally as the only possible optimum energy solutions. Though sessile drops have been analyzed for variable contact area,[19] the present approach is

the only one to our knowledge which is valid for pendant drops hanging from a surface on which they can choose the minimum energy. Not only do the possible solutions appear spontaneously and reveal various features of the solution space, the approach can be extended toward analytical solutions for patterned surfaces.

A range of solutions of long drops obtained by earlier workers is shown to consist of unphysical shapes, so at small volumes, a two-dimensional drop has a unique static shape. This is confirmed analytically by showing that the maximum height achievable by a static two-dimensional drop is $3.42L_c$. It is obtained numerically that axisymmetric drops, on the other hand, can be infinitely long, but their volume must remain finite. While a two-dimensional drop can have, at most, two static solutions of a given volume, an axisymmetric drop can adopt infinitely many shapes. A range of longer two-dimensional drops is found to be of minimum energy in a one-dimensional space of Lagrange multipliers and stable to two-dimensional perturbations. In this range, for a given contact angle, the drop height decreases with increasing volume, while the contact area with the solid surface increases. There is thus an additional bifurcation curve between unstable and stable solutions, corresponding to minimum contact area shapes. In axisymmetric drops, over a small range of volume, repeated sets of left and right Y limbs are possible, with repeating regions of minimum and maximum energy separated by bifurcation curves. The dynamics of these drops when subjected to forces, as well as their stability to three-dimensional perturbations, are being studied.

ACKNOWLEDGMENTS

We are very grateful to Professor B. Andreotti and Professor Rajaram Nityananda for a critical reading of the manuscript and very insightful comments.

APPENDIX: ENERGY MINIMIZATION

The extremization of a functional with variable end points is conducted in the standard manner prescribed, for example, by Brunt.[20] We give here the essential steps toward obtaining Eqs. (3)–(6).

The functional E_0 must be extremized subject to the constraint of constant volume V, i.e., the first variation of

$$E_0 = \int_{z=0}^{z=h} G(z,x,x_z)\mathrm{d}z + \chi V \tag{A1}$$

with respect to $x(z)$ must be zero. Here $V=\int_0^h x\mathrm{d}z$ is referred to as volume, as per convention. χ is the Lagrange multiplier, x_z denotes $\mathrm{d}x/\mathrm{d}z$, and

$$G \equiv \sqrt{1+x_z^2} + \frac{\gamma_{sl}-\gamma_{sg}}{\gamma}x_z + xz - V - \chi x. \tag{A2}$$

We consider a perturbed shape $\hat{x}=x+\epsilon\eta(z)$, where ϵ is a small parameter. We prescribe that the bottom tips of the perturbed and the original drops coincide, as seen in Fig. 1. Let the corresponding changes in the end points be $[\hat{\lambda}=\lambda+\epsilon\Lambda,\ \hat{h}=h+\epsilon H]$.

The energy minimization functional defined as

$$E(\hat{x}) - E(x) = \int_0^{h+\epsilon H} G(z,\hat{x},\hat{x}_z)\mathrm{d}z - \int_0^h G(z,x,x_z)\mathrm{d}z.$$

After a few mathematical manipulations, we get

$$E_0(\hat{x}) - E_0(x) = \epsilon\left\{\int_0^h \eta\left[\frac{\partial G}{\partial x} - \frac{\mathrm{d}}{\mathrm{d}z}\left(\frac{\partial G}{\partial x_z}\right)\right]\mathrm{d}z + \left[\Lambda\frac{\partial G}{\partial x_z} + H\left(G - x_z\frac{\partial G}{\partial x_z}\right)\right]\Bigg|_{z=h}\right\}. \tag{A3}$$

For the functional E_0 to be stationary at $x(z)$, terms of $O(\epsilon)$ should add to zero in the above expression. The perturbation $\eta(z)$ can be chosen arbitrarily, which demands that the integrand be zero. This gives the Euler–Lagrange Eq. (3). A hydrostatic force balance indicates that $\chi=1/r_0$, where r_0 is the radius of curvature at the origin, assigning a physical meaning to the Lagrange's multiplier. Defining $\cot\theta \equiv x_z$, Eq. (3) can be written as

$$z = \left(\frac{1}{r_0} - \cos\theta\frac{\mathrm{d}\theta}{\mathrm{d}x}\right). \tag{A4}$$

To satisfy Eq. (A3), in addition to the force balance, we must have

$$\left[\left(\frac{\epsilon\Lambda}{\epsilon H} - x_z\right)\frac{\partial G}{\partial x_z} + G\right]\Bigg|_{z=h} = 0, \tag{A5}$$

assuming $\epsilon H \neq 0$.

Noting that the volume may be expressed as[7]

$$V = h\lambda - \frac{\lambda}{r_0} + \sin\theta_s, \tag{A6}$$

where $\cot(\theta_s)$ is the slope x_z at the solid surface, we get Eq. (4) as the boundary condition.

For axisymmetric pendant drops, the energy functional (Fig. 1), will have the same form as in Eq. (A1) but with

$$G \equiv 2\pi r\left[\sqrt{1+r_z^2} + \frac{\gamma_{sl}-\gamma_{sg}}{\gamma}r_z\right] + \pi r^2\left[z - \frac{1}{r_0}\right] - V. \tag{A7}$$

The appropriate value of the Lagrange multiplier has been used. In this case, volume may be determined as

$$V = \pi R^2 h - \pi R\left[\frac{R}{r_0} - 2\sin\theta_s\right]. \tag{A8}$$

As before, Eqs. (5) and (6) can be recovered.

[1] R. Finn, Not. Am. Math. Soc. **46**, 770 (1999).
[2] J. A. F. Plateau, *Statique Experimentale et Theorique des Liquides Soumis aux Seules Forces Molculaires* (Gauthier-Villars, Paris, 1873).
[3] J. C. Adams and F. Bashforth, *An Attempt to Test the Theories of Capillary Action by Comparing the Theoretical and Measured Forms of Drops of Fluid* (Cambridge University Press, Cambridge, 1883).
[4] W. Thomson (Lord Kelvin), Nature (London) **34**, 290 (1886).
[5] J. F. Padday, Philos. Trans. R. Soc. London **269**, 265 (1971).
[6] J. F. Padday and A. R. Pitt, Philos. Trans. R. Soc. London **275**, 489 (1973).
[7] E. Pitts, J. Fluid Mech. **59**, 753 (1973).
[8] E. Pitts, J. Fluid Mech. **63**, 487 (1974).
[9] E. A. Boucher and M. J. B. Evans, Proc. R. Soc. London, Ser. A **346**, 349 (1975).

[10] E. A. Boucher, M. J. B. Evans, and H. J. Kent, Proc. R. Soc. London, Ser. A **349**, 81 (1976).
[11] P. Concus and R. Finn, Proc. R. Soc. London, Ser. A **292**, 307 (1979).
[12] S. R. Majumdar and D. H. Michael, Proc. R. Soc. London, Ser. A **351**, 89 (1976).
[13] D. H. Michael and P. G. Willaims, Proc. R. Soc. London, Ser. A **351**, 117 (1976).
[14] D. H. Michael, Annu. Rev. Fluid Mech. **13**, 189 (1981).
[15] H. C. Wente, Pac. J. Math. **88**, 421 (1980).
[16] A. K. Chesters, J. Fluid Mech. **81**, 609 (1977).
[17] S. B. G. O'Brien, J. Fluid Mech. **233**, 519 (1991).
[18] S. B. G. O'Brien, SIAM J. Appl. Math. **62**, 1569 (2002).
[19] J. H. Snoeijer and B. Andreotti, Phys. Fluids **20**, 057101 (2008).
[20] B. van Brunt, *The Calculus of Variations* (Springer-Verlag, New York, 2004).
[21] P.G. de Gennes, F. Brochard-Wyart, and D. Quere, *Capillarity And Wetting Phenomena: Drops, Bubbles, Pearls, Waves* (Springer, New York, 2004).
[22] B. Krasovitski and A. Marmur, Langmuir **21**, 3881 (2005).
[23] P. S. Swain and R. Lipowsky, Langmuir **14**, 6772 (1998).
[24] G. Wolansky and A. Marmur, Colloids Surf., A **156**, 381 (1999).